
Article:
Liu, W. and Hawes, M.B. (2014) Sparse Array Design for Wideband Beamforming with Reduced Complexity in Tapped Delay-lines. IEEE Transactions on Audio, Speech and Language Processing, 22 (8). pp. 1236-1247. ISSN 1558-7916

https://doi.org/10.1109/TASLP.2014.2327298

Sparse Array Design for Wideband Beamforming with Reduced Complexity in Tapped Delay-lines

Matthew B. Hawes and Wei Liu
Communications Research Group
Department of Electronic and Electrical Engineering
University of Sheffield, UK
{elp10mbh, w.liu}@sheffield.ac.uk

***Abstract*—Sparse wideband array design for sensor location optimisation is highly nonlinear and it is traditionally solved by genetic algorithms (GAs) or other similar optimization methods. This is an extremely time-consuming process and an optimum solution is not always guaranteed. In this work, this problem is studied from the viewpoint of compressive sensing (CS). Although there have been CS-based methods proposed for the design of sparse narrowband arrays, its extension to the wideband case is not straightforward, as there are multiple coefficients associated with each sensor and they have to be simultaneously minimised in order to discard the corresponding sensor locations. At first, sensor location optimisation for both general wideband beamforming and frequency invariant beamforming is considered. Then, sparsity in the tapped delay-line (TDL) coefficients associated with each sensor is considered in order to reduce the implementation complexity of each TDL. Finally, design of robust wideband arrays against norm-bounded steering vector errors is addressed. Design examples are provided to verify the effectiveness of the proposed methods, with comparisons drawn with a GA-based design method.**

***Index Terms*—Sparse array, frequency invariant beamforming, wideband beamforming, robust beamforming, compressive sensing, implementation complexity.**

I. Introduction

Wideband beamforming has been studied extensively in the past [1], [2], [3], [4], [5], [6]. It is well-known that in order to avoid the spatial aliasing problem for uniform linear arrays (ULAs), the adjacent sensor spacing has to be less than half of the minimum operating wavelength corresponding to the highest frequency of the signal of interest. This can be problematic when considering arrays with a large aperture size, due to the cost associated with the number of sensors required. As a result, sparse arrays, which allow adjacent sensor separations greater than half a wavelength while still avoiding grating lobes due to the randomness of sensor locations, are a desirable alternative [7]. Moreover, even with the same number of sensors and a similar aperture size, the nonuniform nature of a sparse array also provides more degrees of freedom to achieve a better beam response.

However, the unpredictable sidelobe behaviour associated with sparse arrays means some optimisation of sensor locations is required to reach an acceptable performance level. Various nonlinear methods have been used to achieve this required optimisation. For example, Genetic Algorithms (GAs) [8], [9], [10], [11], [12], [13], Simulated Annealing (SA) [14], [15]. In particular, in [16], the wideband sparse array design problem is studied using an SA-based approach which can result to either a frequency invariant response or a maximum directivity one while controlling the sidelobe level and without the need of setting a desired response in advance. The disadvantage of these types of methods are the potentially extremely long computation times and the possibility of convergence to a non-optimal solution.

Recently, the area of compressive sensing (CS) has been explored [17], and CS-based methods have been proposed in the design of narrowband sparse arrays [18], [19], [20], [21], [22], [23], [24], [25]. CS theory tells us that if certain conditions are met it is possible to recover some signals from fewer measurements than are used by traditional methods. This can then form the basis of sparse array design methods by trying to attain an exact, or almost exact, match to a desired response while using as few sensors as possible. This is achieved by minimising the l_1 norm of the weight coefficients, subject to the error between the desired and designed responses being below a predefined level. Further work has also shown that it is possible to improve the sparseness of a solution by considering a reweighted l_1 minimisation problem [26], [27], [28]. The aim of these methods is to bring the minimisation of the l_1 norm of the weight coefficients closer to that of the minimisation of the l_0 norm, by solving a series of reweighted l_1 minimisations, where locations with small weight coefficients are more heavily penalised than locations with large weight coefficients.

It is not straightforward to extend the design to the wideband case, as there are tapped delay-lines (TDLs) or FIR/IIR filters associated with each received wideband signal, and for a wideband array to be sparse all coefficients along the TDL associated with an individual sensor have to be equal or very close to zero. Therefore, it is not sufficient to simply minimize the l_1 norm of the weight coefficients. Instead all the weight coefficients along a TDL have to be simultaneously minimized. In order to achieve this, a method similar to the technique employed in complex-valued l_1 norm minimization [29], is proposed in this paper, which is a further expansion of the idea presented in [30] by the same authors. As in the case with the reweighted l_1 minimisation method for narrowband array design, it is possible to use a reweighted scheme for the wideband method as well. This involves the reweighting terms being applied to the weight coefficients in the reformulated wideband problem.

A further contribution in this work is the design of sparse frequency invariant beamformers (FIBs) using the CS-based approach. FIB design has been studied in the areas of fixed [31], [32], [33], [34], and adaptive [35], beamforming. Both use the idea of response variation (RV) to account for the difference in response at each frequency to that at the reference frequency in the design process. In this work the RV will be added as a constraint to the reformulated wideband CS problem in an attempt to obtain a sparse FIB.

Another problem of interest is the reduction in complexity of the TDLs or FIR/IIR filters associated with each sensor location. In other words, it is desirable to have as few non-zero coefficients along the TDLs as possible. Similar problems

have been studied in the FIR filter design area [36], [37], [38]. In this work we propose looking at this problem from the view point of CS and to combine it with the traditional problem of finding the minimum number of active sensor locations, with two methods being proposed. Firstly, a fixed set of sensor locations can be found using one of our proposed wideband CS methods. The final coefficients for these fixed locations can then be found by solving a second l_1 minimisation of the weight coefficients. Alternatively, the sparsity in locations and in coefficients along a TDL can be simultaneously maximised. To do this the cost function at the start of the wideband CS reformulation has to be altered. In both cases a reweighted scheme can be derived.

Moreover, one practical issue in the design of wideband arrays is the steering vector error caused by model perturbations such as sensor location errors and individual sensor response discrepancies. Many methods have been proposed for robust design of such arrays, such as constraining the white noise gain [39], [40], using worst-case performance optimisation [41] or considering the probability density functions of the sensor characteristics [16]. In this work we use an extra constraint to limit the effect of norm-bounded steering vector errors [23], [42], which ensures the maximum possible change in array response remains below a predetermined acceptable level, therefore allowing a robust response.

The remainder of this paper is structured as follows. Sec. II gives details of the proposed CS-based design methods for location sparsity, which includes the array model in II-A, the proposed standard CS method in II-B, and derivation of the frequency invariant (FI) constraint for CS in II-C, with II-D showing how the problem can be altered to a reweighted CS problem. Details of two design methods for a lower complexity TDL are shown in Sec. III, with Sec. IV giving details of a constraint that ensure robustness to steering vector errors. Finally, design examples are provided in Sec. V and conclusions drawn in Sec. VI.

II. Proposed Wideband Array Designs for Location Sparsity

A. Wideband Array Model

A general linear array structure for wideband beamforming with a TDL length J is shown in Fig. 1, where T_s is the sampling period or temporal delay between adjacent signal samples [2]. We assume that all of the sensors are omnidirectional with the same response, and the signals impinge upon the array from the far field. The beamformer output $y[n]$ is a linear combination of differently delayed versions of the received array signals $x_m[n]$, $m = 0, \cdots, M-1$. The distance from the zeroth sensor to the subsequent sensor is denoted by d_m for $m = 0, \cdots, M-1$, with $d_0 = 0$. Fig. 1 also shows an incident signal arriving at an angle θ.

The steering vector of the array as a function of the normalized frequency $\Omega = \omega T_s$ and the arrival angle θ is

$$\begin{aligned}\mathbf{s}(\Omega,\theta) &= [1, \cdots, e^{-j\Omega(J-1)}, e^{-j\Omega\mu_1\cos(\theta)}, \\ &\quad e^{-j\Omega(\mu_1\cos(\theta)+1)}, \cdots, e^{-j\Omega(\mu_1\cos(\theta)+(J-1))}, \\ &\quad \cdots, e^{-j\Omega(\mu_{M-1}\cos(\theta)+(J-1))}]^T , \end{aligned} \quad (1)$$

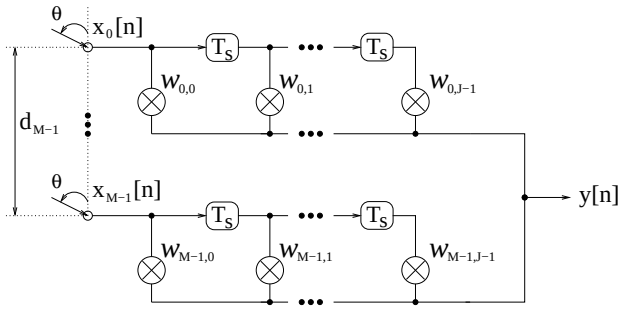

Fig. 1. A general wideband beamforming structure with a TDL length J.

where $\mu_m = \frac{d_m}{cT_s}$ for $m = 0, 1, \cdots, M-1$ and $\{\cdot\}^T$ indicates transpose operation.

The response of the array is then given by

$$P(\Omega,\theta) = \mathbf{w}^H \mathbf{s}(\Omega,\theta), \quad (2)$$

where $\mathbf{w}^H$ is the Hermitian transpose of the weight vector of the array, given by

$$\mathbf{w} = [\mathbf{w}_0^T \ \mathbf{w}_1^T \ \ldots \ \mathbf{w}_{M-1}^T]^T \quad (3)$$

$$\mathbf{w}_m = [\mathrm{w}_{m,0} \ \mathrm{w}_{m,1} \ \ldots \ \mathrm{w}_{m,J-1}]^T . \quad (4)$$

B. Sparse Wideband Array Design via Compressive Sensing

CS has been employed in the design of sparse narrowband arrays by trying to match the array's response to a desired/reference one, $P_r(\Omega,\theta)$. Extending the design to the wideband case, we first consider Fig. 1 as being a grid of potential active sensor locations. In this instance, d_{M-1} is the maximum aperture of the array and the values of d_m, for $m = 1, 2, \ldots, M-2$, are selected to give a uniform grid, with M being a large enough number to cover all potential locations of the sensors. Sparseness is then introduced by selecting the set of weight coefficients to give as few active locations as possible, while still giving a designed response that is close to the desired one.

In the first instance, this problem could be formulated as

$$\min ||\mathbf{w}||_0 \ \text{ subject to } \ ||\mathbf{p}_r - \mathbf{w}^H\mathbf{S}||_2 \leq \alpha \ , \quad (5)$$

where $||\mathbf{w}||_0$ is the number of nonzero coefficients in $\mathbf{w}$, $\mathbf{p}_r$ is the vector holding the desired beam response at sampled frequency points Ω_k and angle θ_l, $k = 0, \cdots, K-1$, $l = 0, \cdots, L-1$, $\mathbf{S}$ is the matrix composed of the steering vectors at the corresponding frequency Ω_k and angle θ_l, α places a limit on the allowed difference between desired and designed responses, and $||.||_2$ denotes the l_2 norm.

In detail, $\mathbf{p}_r$ and $\mathbf{S}$ are respectively given by

$$\begin{aligned}\mathbf{p}_r &= [P_r(\Omega_0,\theta_0), \cdots, P_r(\Omega_0,\theta_{L-1}), P_r(\Omega_1,\theta_0), \\ &\quad \cdots, P_r(\Omega_1,\theta_{L-1}), \cdots, P_r(\Omega_{K-1},\theta_{L-1})] \end{aligned} \quad (6)$$

and

$$\begin{aligned}\mathbf{S} &= [\mathbf{s}(\Omega_0,\theta_0), \cdots, \mathbf{s}(\Omega_0,\theta_{L-1}), \mathbf{s}(\Omega_1,\theta_0), \\ &\quad \cdots, \mathbf{s}(\Omega_1,\theta_{L-1}), \cdots, \mathbf{s}(\Omega_{K-1},\theta_{L-1})] . \end{aligned} \quad (7)$$

Here the desired response $P_r(\Omega,\theta)$ can be obtained from that of a traditional uniform linear array, or simply assumed to be

an ideal response (i.e. one at the mainlobe area and zero for the sidelobe area) and this is adopted in what follows.

In practice, the cost function in (5) will be replaced by the l_1 norm,

$$\min ||\mathbf{w}||_1 \text{ subject to } ||\mathbf{p}_r - \mathbf{w}^H\mathbf{S}||_2 \leq \alpha \ . \tag{8}$$

The above formulation is effective in the design of narrowband arrays, where the TDL length $J = 1$ and the number of nonzero coefficients will be the same as the number of active sensors. In other words, any coefficient with a zero value will mean that the associated sensor is inactive. However, in the wideband case, solving (8) will not guarantee a sparse solution due to there being a TDL length of $J > 1$, with multiple weight coefficients associated with each sensor location. The minimization in (8) only looks to have as few nonzero weight coefficients as possible without considering which TDL they are on.

For a sparse solution, the weight coefficients along a TDL have to be simultaneously minimized. When all coefficients along a TDL are zero-valued, we can then consider the corresponding location to be inactive and sparsity is introduced. To achieve this, we minimize a modified l_1 norm as follows,

$$\begin{aligned} \min \quad & t \ \epsilon \ \mathbb{R}^+ \\ \text{subject to} \quad & ||\mathbf{p}_r - \mathbf{w}^H\mathbf{S}||_2 \leq \alpha \text{ and } |\langle\mathbf{w}\rangle|_1 \leq t \ , \end{aligned} \tag{9}$$

where

$$|\langle\mathbf{w}\rangle|_1 = \sum_{m=0}^{M-1} \left|\left| \begin{bmatrix} w_{m,0} \\ \vdots \\ w_{m,J-1} \end{bmatrix} \right|\right|_2 . \tag{10}$$

Now we decompose t to $t = \sum_{m=0}^{M-1} t_m$, $t_m \epsilon \ \mathbb{R}^+$. In vector form, we have

$$t = [1, \cdots, 1] \begin{bmatrix} t_0 \\ \vdots \\ t_{M-1} \end{bmatrix} = \mathbf{1}^T\mathbf{t}. \tag{11}$$

Then (9) can be rewritten as

$$\begin{aligned} \min_{\mathbf{t}} \quad & \mathbf{1}^T\mathbf{t} \\ \text{subject to} \quad & ||\mathbf{p}_r - \mathbf{w}^H\mathbf{S}||_2 \leq \alpha \\ & \left|\left| \begin{bmatrix} w_{m,0} \\ \vdots \\ w_{m,J-1} \end{bmatrix} \right|\right|_2 \leq t_m, \ \ m = 0, \cdots, M-1. \end{aligned} \tag{12}$$

Now define

$$\hat{\mathbf{w}} = [t_0, w_{0,0}, \cdots, w_{0,J-1}, t_1, \cdots, w_{M-1,J-1}]^T, \tag{13}$$

$$\hat{\mathbf{c}} = [1, \mathbf{0}_J, 1, \mathbf{0}_J, \cdots, \mathbf{0}_J]^T \tag{14}$$

and

$$\begin{aligned} \hat{\mathbf{s}}(\Omega, \theta) \ = \ & [0, 1, \cdots, e^{-j\Omega(J-1)}, \\ & 0, e^{-j\Omega\mu_1\cos(\theta)}, e^{-j\Omega(\mu_1\cos(\theta)+1)}, \cdots, \\ & e^{-j\Omega(\mu_1\cos(\theta)+(J-1))}, \\ & \cdots, e^{-j\Omega(\mu_{M-1}\cos(\theta)+(J-1))}]^T, \end{aligned} \tag{15}$$

where $\mathbf{0}_J$ is an all-zero $1 \times J$ row vector. A matrix $\hat{\mathbf{S}}$ similar to (7) can be created from $\hat{\mathbf{s}}$, given by

$$\begin{aligned} \hat{\mathbf{S}} \ = \ & [\hat{\mathbf{s}}(\Omega_0, \theta_0), \cdots, \hat{\mathbf{s}}(\Omega_0, \theta_{L-1}), \\ & \hat{\mathbf{s}}(\Omega_1, \theta_0), \cdots, \hat{\mathbf{s}}(\Omega_1, \theta_{L-1}), \cdots, \hat{\mathbf{s}}(\Omega_{K-1}, \theta_{L-1})]. \end{aligned}$$

Finally we arrive at the final formulation for the sparse wideband sensor array design problem

$$\begin{aligned} \min_{\hat{\mathbf{w}}} \quad & \hat{\mathbf{c}}^T\hat{\mathbf{w}} \\ \text{subject to} \quad & ||\mathbf{p}_r - \hat{\mathbf{w}}^H\hat{\mathbf{S}}||_2 \leq \alpha \\ & \left|\left| \begin{bmatrix} w_{m,0} \\ \vdots \\ w_{m,J-1} \end{bmatrix} \right|\right|_2 \leq t_m, \ \ m = 0, \cdots, M-1. \end{aligned} \tag{16}$$

C. CS-based Design with Frequency Invariant Constraint

In [33], [34], [35], RV is used as a measure of how close the response at each sampled frequency point is to that at a reference frequency Ω_r. The RV is defined as follows

$$\begin{aligned} RV \ &= \ \sum_{\Omega_I} \sum_{\Theta_{FI}} |\hat{\mathbf{w}}^H\hat{\mathbf{s}}(\Omega, \theta) - \hat{\mathbf{w}}^H\hat{\mathbf{s}}(\Omega_r, \theta)|^2 \\ &= \ \hat{\mathbf{w}}^H\mathbf{Q}\hat{\mathbf{w}} \end{aligned} \tag{17}$$

where

$$\mathbf{Q} = \sum_{\Omega_I} \sum_{\Theta_{FI}} (\hat{\mathbf{s}}(\Omega, \theta) - \hat{\mathbf{s}}(\Omega_r, \theta))(\hat{\mathbf{s}}(\Omega, \theta) - \hat{\mathbf{s}}(\Omega_r, \theta))^H, \tag{18}$$

Θ_{FI} is the angular range over which RV is calculated, and the normalised frequency range of interest, Ω_I, is sampled K times. If $RV = 0$, it implies that the responses at each sampled frequency point are the same.

To obtain an FI solution, we first limit the value of RV to a small value σ^2 as follows

$$RV \leq \sigma^2 \ . \tag{19}$$

This can be simplified to

$$RV = ||\mathbf{L}^T\hat{\mathbf{w}}||_2^2 \leq \sigma^2 \ , \tag{20}$$

where $\mathbf{L} = \mathbf{V}\mathbf{U}^{1/2}$, $\mathbf{U}$ is a diagonal matrix containing the eigenvalues of $\mathbf{Q}$, and $\mathbf{V}$ the corresponding eigenvectors. With this added as an extra constraint, (16) changes to

$$\begin{aligned} \min_{\hat{\mathbf{w}}} \quad & \hat{\mathbf{c}}^T\hat{\mathbf{w}} \\ \text{subject to} \quad & ||\mathbf{p}_r - \hat{\mathbf{w}}^H\hat{\mathbf{S}}||_2 \leq \alpha \\ & \left|\left| \begin{bmatrix} w_{m,0} \\ \vdots \\ w_{m,J-1} \end{bmatrix} \right|\right|_2 \leq t_m, \ \ m = 0, \cdots, M-1 \\ & ||\mathbf{L}^T\hat{\mathbf{w}}||_2 \leq \sigma. \end{aligned} \tag{21}$$

However, if Θ_{FI} is set as $[0°, 180°]$, i.e., we want to achieve a frequency invariant response over the whole angle range of the array, then it is not necessary to match the response at each sampled frequency to the ideal response in the formulation, as the response at each frequency should be the same as, or very

similar to, the response at the reference frequency. As a result, only the reference frequency has to be matched to the ideal response, reducing the complexity of the problem. Thus, when $\Theta_{FI} = [0°, 180°]$ we can define $\mathbf{p}_r$ and $\hat{\mathbf{S}}$ as

$$\begin{aligned} \mathbf{p}_r &= [P_r(\Omega_r, \theta_0), \cdots, P_r(\Omega_r, \theta_{L-1})] \\ \hat{\mathbf{S}} &= [\hat{\mathbf{s}}(\Omega_r, \theta_0), \cdots, \hat{\mathbf{s}}(\Omega_r, \theta_{L-1})]. \end{aligned}$$

D. Sparse Array Design via Reweighted Compressive Sensing

In our previous formulations, we have replaced the l_0 norm by the l_1 norm in the cost function. However, we need to note that the l_0 norm would uniformly penalise all non-zero valued coefficients, while the l_1 norm penalises larger non-zero values more heavily than those smaller non-zero values. As a result, we want to alter the original minimisation problem in order to get closer to the uniform penalisation of the original l_0 minimisation. To achieve this, we can introduce a larger weighting term to those coefficients with smaller non-zero values and a smaller weighting term to those coefficients with larger non-zero values. This weighting term will change according to the resultant coefficients at each iteration. This idea then leads to the reweighted l_1 minimization [26].

The reweighted l_1 minimisation has been employed in the design of sparse narrowband arrays [27], [28]. In such a design, the standard l_1 minimisation in (8) is altered to

$$\min \sum_{m=0}^{M-1} a_m^i |w_m^i| \text{ subject to } ||\mathbf{p}_r - \mathbf{w}^H \mathbf{S}||_2 \leq \alpha \ , \qquad (22)$$

where $a_m^i = (|w_m^{i-1}| + \varepsilon)^{-1}$ is the reweighting term and i is the iteration index. The value $\epsilon > 0$ is required to provide numerical stability and it is chosen to be slightly less than the minimum weight coefficient that will be implemented in the final design. Clearly, the way a_m^i is found means a large coefficient gives a small reweighting term, implying the coefficient will remain non-zero valued in the next iteration. However a small non-zero valued coefficient will lead to a large reweighting term. As a result, it is likely that the coefficient will be zero-valued in the next iteration. Therefore, the problem penalise all non-zero valued coefficients in a more uniform manner, leading to a better approximation to l_0 norm minimisation.

Although we can not apply this scheme directly to our modified l_1 minimisation problem, we can borrow the idea and alter the reweighting parameter in order to achieve the same goal. This leads to (21) being altered to

$$\begin{aligned} \min_{\hat{\mathbf{w}}} \quad & \hat{\mathbf{c}}^T \hat{\mathbf{w}} \\ \text{subject to} \quad & ||\mathbf{p}_r - \hat{\mathbf{w}}^H \hat{\mathbf{S}}||_2 \leq \alpha \\ & a_m^i \left|\left| \begin{bmatrix} w_{m,0}^i \\ \vdots \\ w_{m,J-1}^i \end{bmatrix} \right|\right|_2 \leq t_m^i, \\ & \qquad m = 0, \cdots, M-1 \\ & ||\mathbf{L}^T \hat{\mathbf{w}}||_2 \leq \sigma \end{aligned} \qquad (23)$$

where

$$\hat{\mathbf{w}} = [t_0^i, w_{0,0}^i, \cdots, w_{0,J-1}^i, t_1^i, \cdots, w_{M-1,J-1}^i]^T, \qquad (24)$$

$$\hat{\mathbf{c}} = [a_0^i, \mathbf{0}_J, a_1^i, \mathbf{0}_J, \cdots, \mathbf{0}_J]^T \qquad (25)$$

and the reweighting term a_m^i is modified as follows based on the overall contribution of the coefficients along each TDL

$$a_m^i = \left(\left|\left| \begin{bmatrix} w_{m,0}^{i-1} \\ \vdots \\ w_{m,J-1}^{i-1} \end{bmatrix} \right|\right|_2 + \epsilon \right)^{-1}. \qquad (26)$$

Here ϵ is chosen to be slightly less than the overall sensor location contribution threshold that is used to decide whether the location should be considered active or not in the final solution.

The reweighted problem in (23) is iteratively solved as detailed in the steps given below.

1) Set $i = 1$ and obtain an initial estimate of the weight coefficients by solving (21).
2) $i = i + 1$, and find the reweighting terms a_m^i for all m.
3) Solve (23).
4) Repeat steps 2 to 3 until the number of active sensor locations has remained constant for three iterations of the algorithm. We can choose a value larger than three to make sure the iterative process has reached a stable state. However, this would be at the expense of a larger computation time.

As with the narrowband case this method would be expected to give a better sparsity in terms of sensor locations compared to the the non-reweighted method. However, both should successfully introduce some level of the desired sparsity, with the iterative nature of the reweighted minimisation problem causing an increase in the computation time.

III. Sparse TDL Designs for Further Reduced Complexity

The next problem to consider is the reduction in complexity of the TDL, i.e., we also introduce sparsity along the TDL of active sensor locations, so that a smaller number of non-zero coefficients are needed for implementing each TDL. Two methods of achieving this are presented below. Firstly, using a fixed set of sensor locations derived from the earlier methods, it is possible to find the coefficients with the minimum number of non-zero values via a second l_1 minimisation. Secondly, the problem of TDL sparsity can be combined into a reformulated problem so that both location sparsity and TDL sparsity are simultaneously maximised.

A. TDL Sparsity for Fixed Sparse Sensor Locations

From solving either (21) or (23), a set of fixed sensor locations and a first estimate of their associated weight coefficients can be found. The problem now is to consider the introduction of sparsity along the TDL associated with each active sensor location. In other words, we want to find the overall set of weight coefficients with the minimum number of non-zero values. This will give us the lowest possible complexity in terms of the TDLs or FIR/IIR filters associated with each active sensor location.

In the first instance, this problem can be formulated as

$$\begin{aligned} \min \quad & ||\mathbf{w}||_1 \\ \text{subject to} \quad & ||\mathbf{p}_r - \mathbf{w}^H\mathbf{S}||_2 \leq \alpha \ \ \& \ \ ||\mathbf{L}^T\mathbf{w}||_2 \leq \sigma. \end{aligned} \quad (27)$$

Here the values of α and σ are found by evaluating $||\mathbf{p}_r - \mathbf{w}^H\mathbf{S}||_2$ and $||\mathbf{L}^T\mathbf{w}||_2$, for the obtained fixed sensor locations and their associated first estimate of the weight coefficients $\mathbf{w}$.

This can then be reformulated as a reweighted l_1 minimisation problem as follows

$$\begin{aligned} \min \quad & \sum_{m=1}^{M} a_m^i |w_m^i| \\ \text{subject to} \quad & ||\mathbf{p}_r - \mathbf{w}^H\mathbf{S}||_2 \leq \alpha \ \ \& \ \ ||\mathbf{L}^T\mathbf{w}||_2 \leq \sigma \ , \end{aligned} \quad (28)$$

where $a_m^i = (|w_m^{i-1}| + \epsilon)^{-1}$, with ϵ being the minimum value of weight coefficient that will be implemented. This is then iteratively solved using the steps as detailed in Sec. II-D to find the final set of weight coefficients for the fixed sensor locations.

Now the whole proposed method involves two l_1 minimisations: the first is to obtain the active sensor locations via (21) or (23) and the second is to obtain the sparse TDLs via (28). On the other hand, in some situations it may be advantageous to simultaneously consider the sparsity in sensor locations and along TDLs, removing the need for this extra l_1 minimisation. One method of doing this is detailed below.

B. Simultaneously Maximising Location and TDL Sparsities

To simultaneously consider both sparsity in sensor locations and sparsity along the TDLs, as a starting point we transform (9) back into

$$\min |\langle \mathbf{w} \rangle|_1 \ \text{ subject to } \ ||\mathbf{p}_r - \mathbf{w}^H\mathbf{S}||_2 \leq \alpha \ . \quad (29)$$

To reduce the number of non-zero valued coefficients as well as the number of active sensor locations, we alter the cost function in (29) into the following form

$$\begin{aligned} \min \quad & \beta|\langle \mathbf{w} \rangle|_1 + (1-\beta)||\mathbf{w}||_1 \\ \text{subject to} \quad & ||\mathbf{p}_r - \mathbf{w}^H\mathbf{S}||_2 \leq \alpha \ , \end{aligned} \quad (30)$$

where β is a weighting function that determines the relative importance of the two terms in the cost function of (30). It is worth noting that it is the addition of the second term, $||\mathbf{w}||_1$, that introduces the TDL sparsity to the solution. This is because it looks to minimise the overall number of non-zero valued coefficients without considering which TDL they are on. As a result we can have zero valued coefficients on TDLs which have not been made inactive via the minimisation of the modified l_1 norm.

Equation (30) can then be written as

$$\begin{aligned} \min \quad & t \ \epsilon \ \mathbb{R}^+ \\ \text{subject to} \quad & ||\mathbf{p}_r - \mathbf{w}^H\mathbf{S}||_2 \leq \alpha \\ & \beta|\langle \mathbf{w} \rangle|_1 + (1-\beta)||\mathbf{w}||_1 \leq t. \end{aligned} \quad (31)$$

By using the previous definitions of $\hat{\mathbf{w}}$, $\hat{\mathbf{c}}$, $\hat{\mathbf{s}}$ and the decomposition of t, this can be rewritten as

$$\begin{aligned} \min_{\hat{\mathbf{w}}} \quad & \hat{\mathbf{c}}^T\hat{\mathbf{w}} \\ \text{subject to} \quad & ||\mathbf{p}_r - \hat{\mathbf{w}}^H\hat{\mathbf{S}}||_2 \leq \alpha \\ & \beta||\mathbf{w}_m||_2 + (1-\beta)||\mathbf{w}_m||_1 \leq t_m, \\ & \qquad m = 0, \cdots, M-1 \\ & ||\mathbf{L}^T\hat{\mathbf{w}}||_2 \leq \sigma, \end{aligned} \quad (32)$$

where the FI constraint has again been added in an attempt to ensure an FI response is achieved.

Again, this can be reformulated as a reweighted problem which can then be iteratively solved using the steps detailed in Sec. II-D. This gives

$$\begin{aligned} \min_{\hat{\mathbf{w}}} \quad & \hat{\mathbf{c}}^T\hat{\mathbf{w}} \\ \text{subject to} \quad & ||\mathbf{p}_r - \hat{\mathbf{w}}^H\hat{\mathbf{S}}||_2 \leq \alpha \\ & a_m^i(\beta||\mathbf{w}_m||_2 + (1-\beta)||\mathbf{w}_m||_1 \leq t_m), \\ & \qquad m = 0, \cdots, M-1 \\ & ||\mathbf{L}^T\hat{\mathbf{w}}||_2 \leq \sigma, \end{aligned} \quad (33)$$

where

$$\hat{\mathbf{w}} = [t_0^i, w_{0,0}^i, \cdots, w_{0,J-1}^i, t_1^i, \cdots, w_{M-1,J-1}^i]^T \quad (34)$$

$$\hat{\mathbf{c}} = [a_0^i, \mathbf{0}_J, a_1^i, \mathbf{0}_J, \cdots, \mathbf{0}_J]^T, \quad (35)$$

$$\mathbf{w}_m = [w_{m,0}^i, \cdots, w_{m,J-1}^i]^T \quad (36)$$

$$a_m^i = (\beta||\mathbf{w}_m^{i-1}||_2 + (1-\beta)||\mathbf{w}_m^{i-1}||_1 + \epsilon)^{-1} \quad (37)$$

with ϵ being a small value as before.

It is worth noting that here the reweighting scheme is only expected to help with location sparsity and not sparsity along the TDLs, because there is no individual reweighting term for each coefficient along a TDL, and a smaller coefficients will not receive the extra penalty as in [26].

It is reasonable to assume that decreasing β increases the importance of reducing the TDL complexity compared to location sparsity. However, it is hard to exactly predict what the effect will be, as reducing the number of active locations also removes weight coefficients, therefore also contributes to the second term in the reformulated constraint. Similar can be said for removing more coefficients potentially leading to a sensor location becoming inactive.

IV. Robustness to Steering Vector Error Constraint

So far we have assumed a perfectly known array model. In this section, we develop a robust design method against norm-bounded steering vector errors by adding an extra constraint to the existing formulations.

Suppose the actual steering vector is given by

$$\tilde{\mathbf{s}} = \mathbf{s} + \mathbf{e}, \quad (38)$$

where $\tilde{\mathbf{s}}$ is the actual steering vector, $\mathbf{s}$ is the designed steering vector and $\mathbf{e}$ is the corresponding error vector, which is assumed to be norm-bounded, i.e.,

$$||\mathbf{e}||_2 \leq \varepsilon \ . \quad (39)$$

With this we can find the maximum possible change in array response due to the error as follows

$$|\mathbf{w}^H\tilde{\mathbf{s}} - \mathbf{w}^H\mathbf{s}| = |\mathbf{w}^H\mathbf{e}| \leq \varepsilon||\mathbf{w}||_2 \ . \tag{40}$$

This change in response can be kept below a predetermined acceptable value, i.e.

$$\varepsilon||\mathbf{w}||_2 \leq \gamma \tag{41}$$

where γ is the limit on the allowed change.

Adding (41) to the reweighted problem in (23) we obtain

$$\begin{aligned} \min_{\hat{\mathbf{w}}} \quad & \hat{\mathbf{c}}^T\hat{\mathbf{w}} \\ \text{subject to} \quad & ||\mathbf{p}_r - \hat{\mathbf{w}}^H\hat{\mathbf{S}}||_2 \leq \alpha \\ & a_m^i \left|\left| \begin{bmatrix} w_{m,0}^i \\ \vdots \\ w_{m,J-1}^i \end{bmatrix} \right|\right|_2 \leq t_m^i, \\ & \qquad m = 0, \cdots, M-1 \\ & ||\mathbf{L}^T\hat{\mathbf{w}}||_2 \leq \sigma \ , \ \varepsilon||\mathbf{w}||_2 \leq \gamma \ . \end{aligned} \tag{42}$$

The solution to (42) will give a set of locations and TDL coefficients to implement a robust FIB.

Based on the set of robust sensor locations obtained before, to find a set of temporally sparse coefficients we consider the following problem

$$\begin{aligned} \min_{\mathbf{w}} \quad & ||\mathbf{w}||_1 \\ \text{subject to} \quad & ||\mathbf{p}_r - \mathbf{w}^H\mathbf{S}||_2 \leq \alpha \\ & ||\mathbf{L}^T\mathbf{w}||_2 \leq \sigma \ , \ \varepsilon||\mathbf{w}||_2 \leq \gamma. \end{aligned} \tag{43}$$

where the FI constraint is applied over $\Theta_{FI} = [0°, 180°]$, and

$$\mathbf{p}_r = [P_r(\Omega_r, \theta_0), \cdots, P_r(\Omega_r, \theta_{L-1})] \tag{44}$$

$$\mathbf{S} = [\mathbf{s}(\Omega_r, \theta_0), \cdots, \mathbf{s}(\Omega_r, \theta_{L-1})] \ . \tag{45}$$

Here the values of α, σ and γ can be found by evaluating $||\mathbf{p}_r - \mathbf{w}^H\mathbf{S}||_2, ||\mathbf{L}^T\mathbf{w}||_2$ and $\varepsilon||\mathbf{w}||_2$ from the solution to (42).

V. Design Examples

In this section broadside and off-broadside design examples will be presented, which were all implemented on a computer with an Intel Core Duo CPU E6750 (2.66GHz) and 4GB of RAM. This was done using cvx, a package for specifying and solving convex programs [43], [44].

For all design examples, sensor locations with negligible contributions to the overall response were discarded and active locations on directly adjacent grid locations were merged to their midpoint. As a result, the final weight coefficients may no longer be optimal for the final sensor locations. However, when sparsity along a TDL is not being considered, the locations will allow the effective design of an FIB using the constrained least squares (CLS) formulation as detailed in [34], with a value $\beta_{CLS} = 0.01$ selected, as briefed in the following.

The CLS design minimises a cost function J_{CLS}, subject to a given constraint

$$\min_{\mathbf{w}} J_{CLS} = \mathbf{w}^H\mathbf{Q}_{CLS}\mathbf{w} \text{ subject to } \mathbf{C}^H\mathbf{w} = \mathbf{f} \ , \tag{46}$$

where

$$\begin{aligned} \mathbf{Q}_{CLS} = & \sum_{k=0}^{K-1}\sum_{l=0}^{L-1}(\mathbf{s}(\Omega_k, \theta_l) - \mathbf{s}(\Omega_r, \theta_l)) \\ & (\mathbf{s}(\Omega_k, \theta_l) - \mathbf{s}(\Omega_r, \theta_l))^H + \beta_{CLS}\sum_{\theta_l \in \Theta_s}\mathbf{S}(\Omega_r, \theta_l) \ , \end{aligned} \tag{47}$$

$\mathbf{C} = \mathbf{s}(\Omega_r, \theta_m)$, $\mathbf{f} = 1$, $\mathbf{S}(\Omega_r, \theta_l) = \mathbf{s}(\Omega_r, \theta_l)\mathbf{s}(\Omega_r, \theta_l)^H$, Θ_s is the sidelobe region and θ_m is the mainlobe. Its solution is

$$\mathbf{w}_{CLS} = \mathbf{Q}_{CLS}^{-1}\mathbf{C}(\mathbf{C}^H\mathbf{Q}_{CLS}^{-1}\mathbf{C})^{-1}\mathbf{f} \ . \tag{48}$$

However, for the robust design case, the CLS design is not applicable and the following formulation is employed instead

$$\begin{aligned} \min_{\mathbf{w}} \quad & ||\mathbf{p}_r - \mathbf{w}^H\mathbf{S}||_2 \\ \text{subject to} \quad & ||\mathbf{L}^T\mathbf{w}||_2 \leq \sigma \ \ \& \ \ \varepsilon||\mathbf{w}||_2 \leq \gamma \ . \end{aligned} \tag{49}$$

The values of σ and γ are found by evaluating the values of $||\mathbf{L}^T\hat{\mathbf{w}}||_2$ and $\varepsilon||\mathbf{w}||_2$ from the solution to (42), respectively.

When sparsity along a TDL is considered, such a redesign is not possible. As a result, more care has to be given to the selection of the threshold value below which locations will be considered inactive and individual coefficients will be discarded.

Comparisons will be drawn with a GA-based design method, which optimises the locations given a fixed number of sensors. For each potential sensor location solution in the population, the weight coefficients can be found using the CLS formulation, which are then used to find the value of the cost function J_{CLS} and the fitness value is assigned as J_{CLS}^{-1}. The initial population of the GA consists of 30 individuals creating 27 offspring in each generation. A mutation rate of 0.25 and a maximum of 30 generations were also used. When making the performance comparison, the following were considered: mean adjacent sensor separations, $|J_{CLS}|$ and computation time.

In what follows, we only show the design examples from the reweighted CS-based methods, as from our experience with different design examples, the reweighted methods consistently gave a solution with fewer active sensor locations. In addition to this, the desirability of the resulting array response was as good as or even better than for the arrays found using the non-reweighting design methods. However, this was at the cost of an increased computation time due to the iterative nature of the reweighted scheme.

For all examples the value of λ is the wavelength associated with a normalized frequency $\Omega = \pi$. For speech signals and microphones, this is equivalent to a 10 KHz signal (with a sampling frequency of 20 KHz) giving a wavelength of 3.4 cm at a speed of 340 m/s.

A. Broadside Design Example with Location Sparsity Only

For this example, the reference pattern was that of an ideal array with the mainlobe at $\theta_m = 90°$ and sidelobe regions of $\Theta_s = [0°, 80°] \bigcup [100°, 180°]$, which were sampled every $1°$. The frequency range of interest $\Omega_I = [0.5\pi, \pi]$ was sampled every 0.05π, with the reference frequency $\Omega_r = \pi$. A grid of 100 potential sensor locations was spread uniformly over an

TABLE I
SENSOR LOCATIONS FOR THE REWEIGHTED BROADSIDE DESIGN EXAMPLE.

n	d_n/λ	n	d_n/λ	n	d_n/λ	n	d_n/λ
0	1.92	3	3.74	6	5.66	9	7.17
1	2.83	4	4.34	7	6.26	10	8.08
2	3.33	5	5.00	8	6.67		

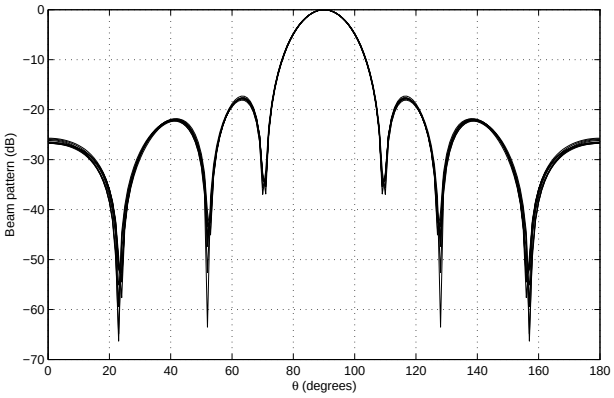

Fig. 2. Responses for reweighted broadside design example.

aperture of 10λ. The values $\alpha = 0.9$, $\sigma = 0.01$, $\epsilon = 9 \times 10^{-4}$ and a TDL length $J = 25$ were used.

The resulting array was made up of 11 active sensor locations as given in Tab. I, with its beam response shown in Fig. 2. It can be seen that the mainlobe is at the desired location for each normalised frequency and sufficient attenuation has been achieved in sidelobe regions. The response also shows a good level of performance in terms of the FI property.

This was then compared to an array designed using the GA-based method. To allow a fair comparison, the GA was set to optimise 11 sensor locations over an aperture of 6.16λ, the same as the example given in Tab. I. Fig. 3 shows the resulting array response and Tab. II gives the locations of each sensor. All these show a good performance in terms of both sidelobe attenuation and the FI property.

Tab. III summarises the different performance measures for each design method. The main disadvantage of the GA design method is clearly shown, i.e. the computation time is significantly longer. This would be even more apparent if a larger population size was used or if more generations were allowed. It is also worth noting that there are more parameters to fine tune with the GA method, for example the mutation rate employed. The mean adjacent sensor spacings are the same in both cases and larger than the spacing of an equivalent ULA, suggesting some sparsity has been achieved. Finally, the value of $|J_{CLS}|$ is slightly lower for reweighted CS design, with the difference largely being the FI property in the extremes of the sidelobe regions. This will not be guaranteed to be the case all the time.

TABLE II
SENSOR LOCATIONS FOR THE GA BROADSIDE DESIGN EXAMPLE.

n	d_n/λ	n	d_n/λ	n	d_n/λ	n	d_n/λ
0	0	3	1.63	6	3.48	9	5.53
1	0.27	4	2.16	7	4.12	10	6.16
2	1.12	5	2.80	8	4.77		

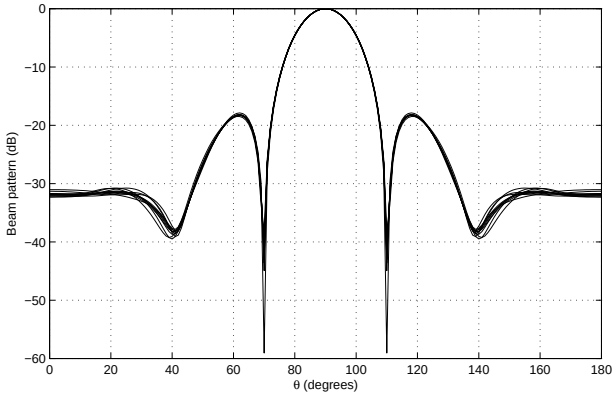

Fig. 3. Responses for the GA broadside design example.

TABLE III
BROADSIDE PERFORMANCE COMPARISON.

Method	Reweighted	GA
Mean Spacing/λ	0.62	0.62
J_{CLS}	0.0372	0.0376
Computation Time (minutes)	130	436

B. Off-Broadside Example with Location Sparsity Only

For this example, the reference pattern was that of an ideal array with the mainlobe at $\theta_m = 125^\circ$ and sidelobe regions of $\Theta_s = [0^\circ, 115^\circ] \bigcup [135^\circ, 180^\circ]$, which were sampled every 1°. The frequency range $\Omega_I = [0.4\pi, 0.9\pi]$ and was sampled every 0.05π, with $\Omega_r = 0.9\pi$ being the reference frequency. A grid of 100 potential sensor locations was spread uniformly over an aperture of 10λ. The values $\alpha = 0.82$, $\sigma = 0.075$, $\epsilon = 9 \times 10^{-4}$ and $J = 25$ were used.

The resulting array consists of 16 active sensor locations over the full aperture of 10λ. The locations are given in Tab. IV and Fig. 4 shows the resulting array response, with its mainlobe at the desired direction and sufficient attenuation in the sidelobe regions. There is also a good level of performance in terms of the FI property.

As with the broadside example, this was compared to an array designed using a GA and result consists of 16 active sensors over an aperture of 10λ as detailed in Tab. V. Fig. 5 shows the corresponding array response, with a satisfactory performance achieved.

Tab. VI summarises the different performance measures for the two arrays. As with the broadside example, the GA design example has taken considerably longer to complete. It

TABLE IV
SENSOR LOCATIONS FOR THE REWEIGHTED OFF-BROADSIDE DESIGN EXAMPLE.

n	d_n/λ	n	d_n/λ	n	d_n/λ	n	d_n/λ
0	0	4	3.03	8	5.25	12	7.58
1	0.51	5	3.54	9	5.86	13	8.08
2	1.92	6	4.14	10	6.46	14	9.49
3	2.42	7	4.75	11	6.97	15	10

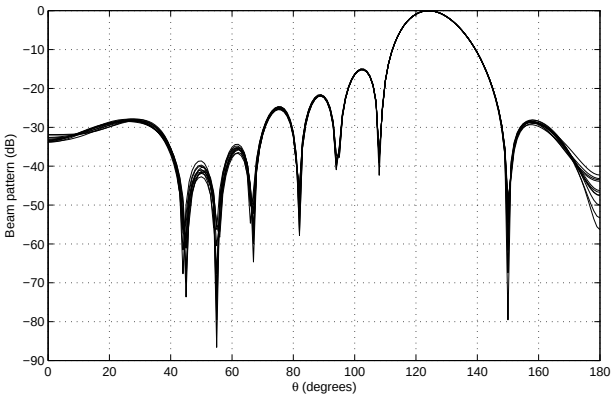

Fig. 4. Responses for the reweighted off-broadside design example.

TABLE V
SENSOR LOCATIONS FOR THE GA OFF-BROADSIDE DESIGN EXAMPLE.

n	d_n/λ	n	d_n/λ	n	d_n/λ	n	d_n/λ
0	0	4	3.16	8	5.08	12	7.23
1	0.78	5	3.37	9	5.84	13	7.78
2	2.27	6	4.16	10	6.31	14	9.16
3	2.63	7	4.75	11	6.77	15	10

is also worth noting that the increase in sensor numbers in this example has led to the computation time being longer than that for the broadside GA design example. Both design methods have given solution arrays with a mean adjacent sensor separation greater than 0.5λ. Unlike for the broadside example, in this case the value of $|J_{CLS}|$ is lower for the GA designed array, suggesting the response is closer to what was desired. This illustrates the fact that although similar performance can be achieved by both design methods, it is hard to predict which will give the best result.

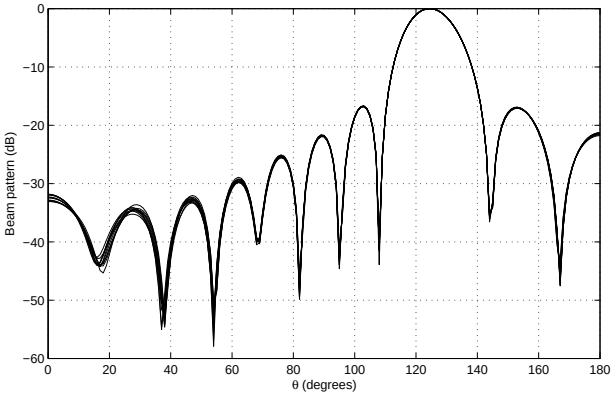

Fig. 5. Responses for the GA off-broadside design example.

TABLE VI
OFF-BROADSIDE PERFORMANCE COMPARISON.

Method	Reweighted	GA
Mean Spacing/λ	0.67	0.66
J_{CLS}	0.0073	0.0062
Computation Time (minutes)	146	944

TABLE VII
BROADSIDE PERFORMANCE COMPARISON FOR TDL SPARSITY.

Method	CLS	Two-Step	Combined
Number of Sensors	11	11	17
Aperture/λ	6.16	6.16	8.38
Mean Spacing/λ	0.62	0.62	0.52
Mean $\|\|\mathbf{w}\|\|_0$ per TDL	25	14.8	18.5
$\|\|\mathbf{p}_r - \mathbf{w}^H\mathbf{S}\|\|_2$	0.900	0.900	0.904
$\|\|\mathbf{L}^T\mathbf{w}\|\|_2$	0.031	0.031	0.098

C. Design Examples Including Sparsity Along the TDLs

Now the performance of the two methods that introduce sparsity along the TDLs will be considered and compared in terms of the number of active sensor locations, overall number of non-zero coefficients, $||\mathbf{p}_r - \mathbf{w}^H\mathbf{S}||_2$ and $||\mathbf{L}^T\mathbf{w}||_2$. Both methods will also be compared to the previous design examples, where we did not consider sparsity along the TDLs. The same threshold scheme was also applied (to remove coefficients with a negligible contribution to the overall response) to these examples here in order to get a fair comparison of performance.

Here we will again only consider the reweighted forms of the two proposed design methods. In addition, we will not consider a comparison with GA here as we have already shown comparable performance levels are reached in our earlier design examples.

1) Broadside Design Examples: For this case, any coefficients with a value below 1×10^{-9} were discarded. For the method involving the second l_1 minimisation of the weight coefficients, the locations found in the previous design example were used. For the combined design method a value of $\beta = 0.8$ was used, along with the same input parameters used in the previous reweighted wideband CS design example. This value was selected in order to ensure that enough importance was still placed on the reduction in the number of sensors, and therefore a sparse solution was still ensured. Tab. VII summarises the performance of the two methods compared to the CLS design example.

The first thing to note is that the introduction of the second term into the modified l_1 minimisation in (33) has lead to there being more active sensor locations. This is to be expected as we are no longer simply trying to minimise the number of active locations but also the number of non-zero valued coefficients. Although the aperture of the array is longer in this case, the mean adjacent sensor separation is smaller due to a larger number of active sensors, suggesting a smaller reduction in number of sensors compared to an equivalent ULA in this instance. In addition, this method also gives a larger average number of coefficients per TDL compared to the two-step method. However, both offer a reduction compared to the design example with coefficients redesigned using the CLS method based on the set of fixed sensor locations.

Comparing the values of $||\mathbf{p}_r - \mathbf{w}^H\mathbf{S}||_2$ and $||\mathbf{L}^T\mathbf{w}||_2$ for the CLS design and the two-step design, we can see that the performance for both measures is the same. However, there is an increase in both values for the combined simultaneous minimisation method. The increase in $||\mathbf{L}^T\mathbf{w}||_2$ is significant, suggesting there will noticeably be an increase in the variation

TABLE VIII
SENSOR LOCATIONS FOR THE BROADSIDE DESIGN EXAMPLE WITH COMBINED MINIMISATION.

n	d_n/λ	n	d_n/λ	n	d_n/λ	n	d_n/λ
0	0.81	4	2.83	8	5.00	12	7.17
1	1.31	5	3.43	9	5.56	13	7.68
2	1.92	6	4.04	10	5.96	14	8.08
3	2.32	7	4.44	11	6.57	15	8.69
						16	9.19

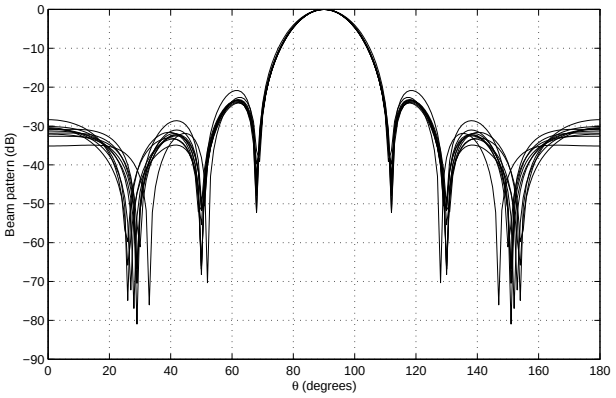

Fig. 6. Responses for the broadside example with two-step minimisation.

between responses at different normalised frequencies. It is likely that this decrease in performance is due to the fact that there is no redesign of the weight coefficients after the merger of sensors on directly adjacent grid locations. The effect of discarding small non-zero valued coefficients is negligible compared to this. As a result, reducing the threshold below which coefficients are discarded will only offer a small improvement, while in some cases drastically increasing the number of non-zero valued coefficients. If improving the final value of $||\mathbf{L}^T\mathbf{w}||_2$ is desirable, then the easiest way would be to put a tighter constraint on the value in the first place.

Figs. 6 and 7 show the response obtained by the two-step l_1 minimisation and combined minimisation methods respectively. For completeness the locations for the combined minimisation are also shown in Tab. VIII.

In both cases the mainlobe is at the correct location of $\theta = 90^\circ$ and there is sufficient sidelobe attenuation. The effect of the increase in the value of $||\mathbf{L}^T\mathbf{w}||_2$ for the combined method can clearly be seen here. The performance in terms of the FI is clearly not as good in the sidelobe regions as it is for the other method. This, coupled with the fact that the two-step method gives us an array with less sensors and less coefficients per sensor, allows us to conclude that the method with the two-step l_1 minimisation is the best of the two.

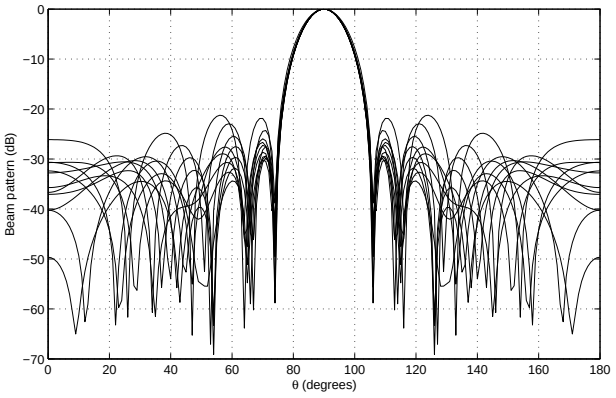

Fig. 7. Responses for the broadside example with combined minimisation.

TABLE IX
OFF-BROADSIDE PERFORMANCE COMPARISON FOR TDL SPARSITY.

Method	CLS	Two-Step
Mean $||\mathbf{w}||_0$ per TDL	25	16.4
$||\mathbf{p}_r - \mathbf{w}^H\mathbf{S}||_2$	0.82	0.82
$||\mathbf{L}^T\mathbf{w}||_2$	0.031	0.075

We could redesign the coefficients for the locations found using the combined minimisation in (33) with another l_1 minimisation as with the first proposed method for TDL sparsity in (28). However, there appears to be no advantage in doing this over using the first method on its own, as the second method in (33) tends to result in more active sensor locations. This would also mean it was unnecessary to include the TDL sparsity in the minimisation in the first place in (33).

2) Off-Broadside Examples: Here we only compare the two-step method in (28) with the CLS redesigned example using the locations obtained by (23), as it has already been shown in the broadside example that the combined minimisation method has no real advantages. Tab. IX summarises the design results of the two methods. Note that the aperture length, number of active locations and mean adjacent separation are not shown, as both have used the same sensor locations.

Here we can see that redesigning the coefficients using an l_1 minimisation has successfully reduced the number of coefficients per sensor location. However, this reduction in the number of coefficients has come at the cost of increasing the final value of $||\mathbf{L}^T\mathbf{w}||_2$. As a result, we would expect more variation in the response at different normalised frequencies. However, there has been no change in the value of $||\mathbf{p}_r - \mathbf{w}^H\mathbf{S}||_2$, suggesting the response at the reference frequency is still as close to the desired response as it previously was. The same criterion for removing small coefficients was applied to both design examples – any TDL coefficient with a value smaller than 1×10^{-6} is discarded. As with the broadside case, this did not change the total number of coefficients that were present for the CLS design example.

D. Robust Sparse Array Design Example

We now consider a broadside design example in order to verify the effectiveness of the method for designing an FIB with robustness against a norm-bounded steering vector error. Here the same parameters as used for the previous broadside design examples are considered. In addition, the values of $\varepsilon = 5$ and $\gamma = 0.0001$ are also used when solving (42).

When deciding if a response is robust or not we randonly generate $N = 1000$ error vectors that meet the norm-bounded constraint in (41). For the n^{th} error vector the achieved response at normalised frequency Ω_k and angle θ_l, $p_n(\Omega_k, \theta_l)$,

TABLE X
SENSOR LOCATIONS FOR THE ROBUST SPARSE ARRAY DESIGN EXAMPLE.

n	d_n/λ	n	d_n/λ n	d_n/λ	n	d_n/λ	
0	1.92	3	3.94	6	5.56	9	7.07
1	2.93	4	4.44	7	6.06	10	8.08
2	3.43	5	5.00	8	6.57		

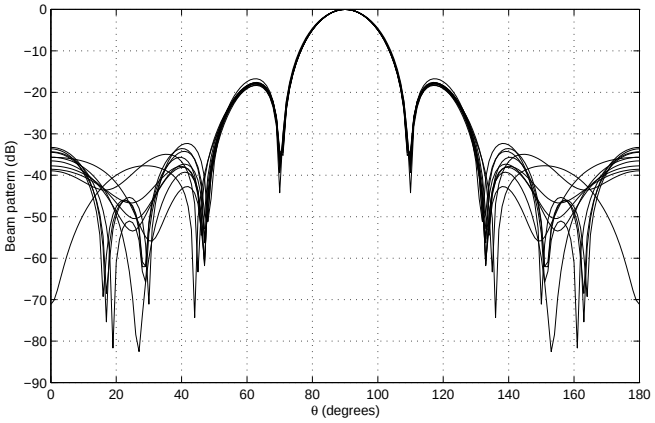

Fig. 8. Designed response without temporal sparsity.

is found and the average achieved response is given by

$$\bar{p}(\Omega_k, \theta_l) = \frac{1}{N} \sum_{n=0}^{N-1} p_n(\Omega_k, \theta_l), \tag{50}$$

which is then used to find the normalised variance of the achieved array response,

$$var(\Omega_k, \theta_l) = \frac{1}{N} \sum_{n=0}^{N-1} \frac{|p_n(\Omega_k, \theta_l) - \bar{p}(\Omega_k, \theta_l)|^2}{|\bar{p}(\Omega_k, \theta_l)|}, \tag{51}$$

A close match between mean achieved and designed responses, along with low normalised variance levels, would indicate that robustness has been achieved.

After discarding negligible locations and merging those on directly adjacent grids we end up with the 11 active sensor locations detailed in Tab. X, giving a mean adjacent sensor separation of 0.62λ. However, this process will again mean the weight coefficients may no longer be optimal for the location we have. The coefficients were however used to find the values $\sigma = 0.035562$ and $\gamma = 0.23732$ that were used solving (49). The result was a set of weight coefficients without zero values (i.e. as expected no TDL sparsity).

Fig. 8 shows the resulting designed response for each of the sampled frequencies. We can see that for each frequency the mainlobe is in the desired location, and sufficient sidelobe attenuation and a good (especially around the mainlobe) FI property is achieved. Fig. 9 shows the mean achieved response, which is a close match to the designed one. Along with the low normalised variance levels shown in Fig. 10, this indicates a robust response has been achieved.

The next one is for designing a temporally sparse robust FIB. With the coefficients obtained in the first step, the values of $\alpha = 0.87448, \sigma = 0.035562$ and $\gamma = 0.23732$ were found for use in solving (43). However, using these constraint values

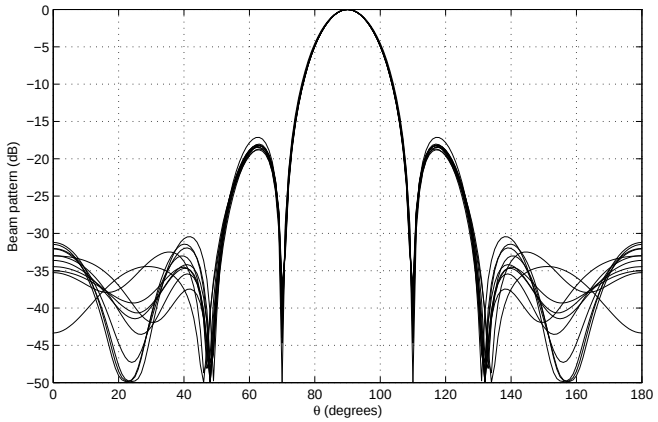

Fig. 9. Mean achieved response without temporal sparsity.

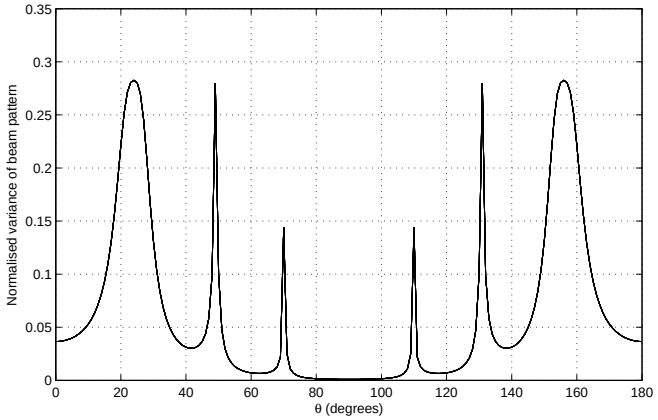

Fig. 10. Normalised variance levels without temporal sparsity.

failed to give a temporally sparse solution. As a result the value of α was increased to 0.9 and a solution showing temporal sparsity was achieved. On average there was a reduction of 13.1 non-zero valued coefficients per TDL.

The designed response, mean achieved response and normalised variance levels are shown in Figs. 11, 12 and 13

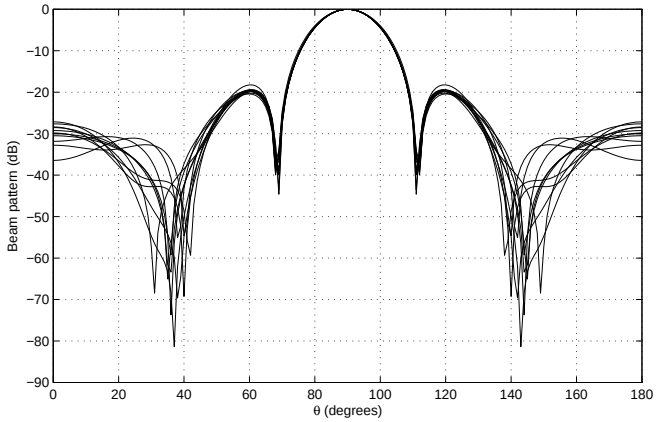

Fig. 11. Designed response with temporal sparsity.

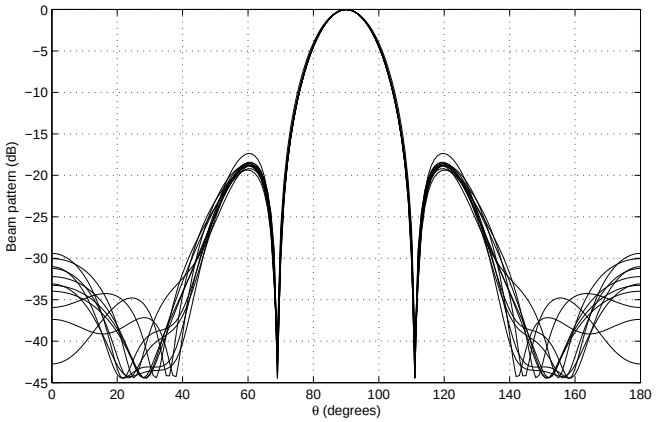

Fig. 12. Mean achieved response with temporal sparsity.

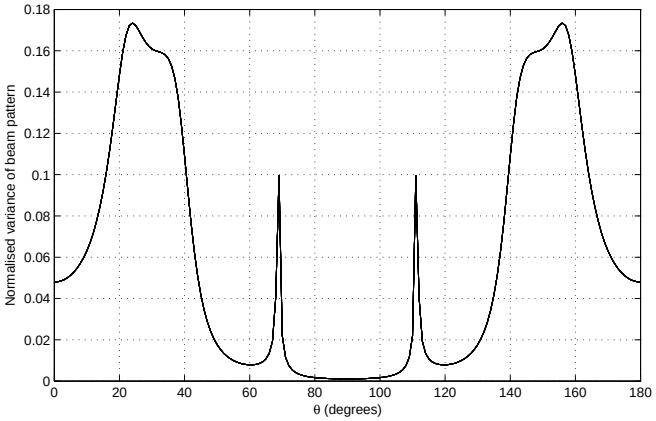

Fig. 13. Normalised variance levels with temporal sparsity.

respectively. Again an acceptable designed response has been achieved, with satisfactory mean achieved response and normalised variance level.

VI. Conclusions

In this paper, a series of CS-based methods for the design of sparse arrays for wideband beamforming including frequency invariant beamforming has been proposed. Two levels of sparsity were considered: one is the sparsity in sensor locations and the other one is the sparsity of the TDL coefficients associated with each sensor in order to reduce the implementation complexity of each TDL.

Although CS-based methods have been proposed for the design of narrowband sparse arrays, their extension to the wideband case is not straightforward, as there are multiple coefficients along a TDL associated with each sensor and it is not sufficient to simply minimize the l_1 norm of the weight vector. Instead all the coefficients along a TDL have to be simultaneously minimized, which was achieved by a modified l_1 norm minimization method. An extra constraint based on the concept of response variation was then added to ensure a frequency invariant response. To further improve the sparsity of array locations, an iterative process is employed with a reweighting term introduced in the cost function so that locations with small contributions are penalised in the next iteration, while locations with a large contribution are replicated.

For the design of sparse TDLs, two methods were proposed. The first one is based on a two-step l_1 minimisation, where we first obtain the sparse sensor locations using the above proposed methods and then find the minimum number of non-zero valued coefficients for the fixed set of sensor locations. In the second method, we consider the sparsity in sensor locations and TDL coefficients simultaneously. It seems that the second one may give a better result. However, based on our design results, the first one has achieved a better result. Details of a further constraint, which can ensure the solution is robust against steering vector errors were also given. This constraint works by keeping the maximum change in array response, due to a norm-bounded steering vector error, below a predetermined acceptable level.

Various design examples have been presented, with comparisons also drawn with a GA-based method. Similar performance levels are achieved but the GA design takes considerably longer to reach the solution, highlighting the advantage of our proposed design methods.

References

[1] M. S. Brandstein and D. Ward, Eds., *Microphone Arrays: Signal Processing Techniques and Applications*. Berlin: Springer, 2001.

[2] W. Liu and S. Weiss, *Wideband Beamforming: Concepts and Techniqeus*. Chichester, UK: John Wiley & Sons, 2010.

[3] S. C. Chan and H. H. Chen, "Uniform concentric circular arrays with frequency-invariant characteristics–theory, design, adaptive beamforming and DOA estimation," *IEEE Transactions on Signal Processing*, vol. 55, pp. 165–177, January 2007.

[4] H. W. Chen and W. Ser, "Design of robust broadband beamformers with passband shaping characteristics using Tikhonov regularization," *IEEE Transactions on Audio, Speech, and Language Processing*, vol. 17, no. 4, pp. 665–681, May 2009.

[5] M. Crocco and A. Trucco, "A computationally efficient procedure for the design of robust broadband beamformers," *IEEE Transactions on Signal Processing*, vol. 58, no. 10, pp. 5420–5424, October 2010.

[6] ——, "Design of robust superdirective arrays with a tunable tradeoff between directivity and frequency-invariance," *IEEE Transactions on Signal Processing*, vol. 59, no. 5, pp. 2169–2181, May 2011.

[7] P. Jarske, T. Saramaki, S. K. Mitra, and Y. Neuvo, "On properties and design of nonuniformly spaced linear arrays," *IEEE Transactions on Acoustics, Speech, and Signal Processing*, vol. 36, no. 3, pp. 372 –380, March 1988.

[8] R. L. Haupt, "Thinned arrays using genetic algorithms," *IEEE Transactions on Antennas and Propagation*, vol. 42, no. 7, pp. 993–999, July 1994.

[9] K.-K. Yan and Y. Lu, "Sidelobe reduction in array-pattern synthesis using genetic algorithm," *IEEE Transactions on Antennas and Propagation*, vol. 45, no. 7, pp. 1117–1122, July 1997.

[10] K. Chen, Z. He, and C. Han, "Design of 2-dimensional sparse arrays using an improved genetic algorithm," in *Proc. IEEE Workshop on Sensor Array and Multichannel Processing*, July 2006, pp. 209–213.

[11] L. Cen, W. Ser, Z. L. Yu, and S. Rahardja, "An improved genetic algorithm for aperiodic array synthesis," in *Proc. IEEE International Conference on Acoustics, Speech, and Signal Processing*, April 2008, pp. 2465 –2468.

[12] M. B. Hawes and W. Liu, "Location optimisation of robust sparse antenna arrays with physical size constraint," *IEEE Antennas and Wireless Propagation Letters*, pp. 1303–1306, November 2012.

[13] Z. Li, K. F. C. Yiu, and Z. Feng, "A hybrid descent method with genetic algorithm for microphone array placement design," *Applied Soft Computing*, vol. 13, no. 3, pp. 1486–1490, 2013.

[14] A. Trucco and V. Murino, "Stochastic optimization of linear sparse arrays," *IEEE Journal of Oceanic Engineering*, vol. 24, no. 3, pp. 291–299, July 1999.

[15] M. R. Bai, J.-H. Lin, and K.-L. Liu, "Optimized microphone deployment for near-field acoustic holography: to be, or not to be random, that is the question," *Journal of Sound and Vibration*, vol. 329, no. 14, pp. 2809–2824, 2010.

[16] M. Crocco and A. Trucco, "Stochastic and analytic optimization of sparse aperiodic arrays and broadband beamformers with robust superdirective patterns," *IEEE Transactions on Audio, Speech, and Language Processing*, vol. 20, no. 9, pp. 2433–2447, Nov 2012.

[17] E. Candes, J. Romberg, and T. Tao, "Robust uncertainty principles: exact signal reconstruction from highly incomplete frequency information," *IEEE Transactions on Information Theory*, vol. 52, no. 2, pp. 489– 509, February 2006.

[18] L. Li, W. Zhang, and F. Li, "The design of sparse antenna array," *CoRR*, vol. arXiv.org/abs/0811.0705, 2008.

[19] G. Prisco and M. D'Urso, "Exploiting compressive sensing theory in the design of sparse arrays," in *Proc. IEEE Radar Conference*, May 2011, pp. 865 –867.

[20] L. Carin, "On the relationship between compressive sensing and random sensor arrays," *IEEE Antennas and Propagation Magazine*, vol. 51, no. 5, pp. 72 –81, October 2009.

[21] G. Oliveri and A. Massa, "Bayesian compressive sampling for pattern synthesis with maximally sparse non-uniform linear arrays," *IEEE Transactions on Antennas and Propagation*, vol. 59, no. 2, pp. 467–481, 2011.

[22] G. Oliveri, M. Carlin, and A. Massa, "Complex-weight sparse linear array synthesis by bayesian compressive sampling," *IEEE Transactions on Antennas and Propagation*, vol. 60, no. 5, pp. 2309–2326, 2012.

[23] M. B. Hawes and W. Liu, "Robust sparse antenna array design via compressive sensing," in *Proc. International Conference on Digital Signal Processing*, 2013.

[24] ——, "Compressive sensing based approach to the design of linear robust sparse antenna arrays with physical size constraint," *IET Microwaves, Antennas & Propagation*, 2014, DOI: 10.1049/iet-map.2013.0469.

[25] ——, "A quaternion-valued reweighted minimisation approach to sparse vector sensor array design," in *Proc. of the International Conference on Digital Signal Processing*, Hong Kong, August 2014.

[26] E. Candes, M. Wakin, and S. Boyd, "Enhancing sparsity by reweighted l_1 minimization," *Journal of Fourier Analysis and Applications*, vol. 14, pp. 877–905, 2008.

[27] B. Fuchs, "Synthesis of sparse arrays with focused or shaped beampattern via sequential convex optimizations," *IEEE Transactions on Antennas and Propagation*, vol. 60, no. 7, pp. 3499 –3503, July 2012.

[28] G. Prisco and M. D'Urso, "Maximally sparse arrays via sequential convex optimizations," *IEEE Antennas and Wireless Propagation Letters*, vol. 11, pp. 192 –195, 2012.

[29] S. Winter, H. Sawada, and S. Makino, "On real and complex valued l_1-norm minimization for overcomplete blind source separation," in *Proc. of IEEE Workshop on Applications of Signal Processing to Audio and Acoustics*, October 2005, pp. 86 – 89.

[30] M. B. Hawes and W. Liu, "Sparse microphone array design for wideband beamforming," in *Proc. International Conference on Digital Signal Processing*, 2013.

[31] W. Liu, S. Weiss, J. G. McWhirter, and I. K. Proudler, "Frequency invariant beamforming for two-dimensional and three-dimensional arrays," *Signal Processing*, vol. 87, pp. 2535–2543, November 2007.

[32] W. Liu and S. Weiss, "Design of frequency invariant beamformers for broadband arrays," *IEEE Transactions on Signal Processing*, vol. 56, no. 2, pp. 855–860, February 2008.

[33] H. Duan, B. P. Ng, C. M. See, and J. Fang, "Applications of the SRV constraint in broadband pattern synthesis," *Signal Processing*, vol. 88, pp. 1035–1045, April 2008.

[34] Y. Zhao, W. Liu, and R. J. Langley, "An application of the least squares approach to fixed beamformer design with frequency invariant constraints," *IET Signal Processing*, vol. 5, pp. 281–291, June 2011.

[35] ——, "Adaptive wideband beamforming with frequency invariance constraints," *IEEE Transactions on Antennas and Propagation*, vol. 59, no. 4, pp. 1175–1184, April 2011.

[36] H.-J. Kang and I.-C. Park, "Fir filter synthesis algorithms for minimizing the delay and the number of adders," *IEEE Transactions on Circuits and Systems II: Analog and Digital Signal Processing*, vol. 48, no. 8, pp. 770–777, 2001.

[37] D. Maskell, "Design of efficient multiplierless fir filters," *IET, Circuits, Devices Systems*, vol. 1, no. 2, pp. 175–180, 2007.

[38] R. Mahesh and A. Vinod, "Low complexity flexible filter banks for uniform and non-uniform channelisation in software radios using coefficient decimation," *IET Circuits, Devices Systems*, vol. 5, no. 3, pp. 232–242, 2011.

[39] E. Mabande, A. Schad, and W. Kellermann, "Design of robust superdirective beamformers as a convex optimization problem," in *Proc. IEEE International Conference on Acoustics, Speech, and Signal Processing*, April 2009, pp. 77–80.

[40] R. Nongpiur and D. Shpak, "L -infinity norm design of linear-phase robust broadband beamformers using constrained optimization," *IEEE Transactions on Signal Processing*, vol. 61, no. 23, pp. 6034–6046, Dec 2013.

[41] H. Chen, W. Ser, and J. Zhou, "Robust nearfield wideband beamformer design using worst case mean performance optimization with passband response variance constraint," *IEEE Transactions on Audio, Speech, and Language Processing*, vol. 20, no. 5, pp. 1565–1572, July 2012.

[42] Y. Zhao and W. Liu, "Robust fixed frequency invariant beamformer design subject to norm-bounded errors," *IEEE Signal Processing Letters*, vol. 20, pp. 169–172, February 2013.

[43] C. Research, "CVX: Matlab software for disciplined convex programming, version 2.0 beta," http://cvxr.com/cvx, September 2012.

[44] M. Grant and S. Boyd, "Graph implementations for nonsmooth convex programs," in *Recent Advances in Learning and Control*, ser. Lecture Notes in Control and Information Sciences, V. Blondel, S. Boyd, and H. Kimura, Eds. Springer-Verlag Limited, 2008, pp. 95–110, http://stanford.edu/ boyd/graph_dcp.html.

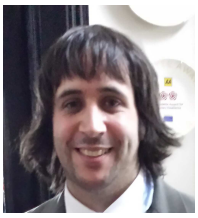

Matthew Hawes was born on The Wirral, United Kingdom, in September 1987. He received his M.Eng degree in Electronic and Communications Engineering from The University of Sheffield in 2010. Since then he has been working towards his Ph.D in the communications research group at the same university. His research interests include sparsity in array signal processing and compressive sensing.

Wei Liu (S'01-M'04-SM'10) received his B.Sc. in Space Physics (minor in Electronics) in 1996, L.L.B. in Intellectual Property Law in 1997, both from Peking University, China, M.Phil. from the Department of Electrical and Electronic Engineering, University of Hong Kong, in 2001, and Ph.D. in 2003 from the School of Electronics and Computer Science, University of Southampton, UK. He then worked as a postdoc in the same group and later in the Communications and Signal Processing Group, Department of Electrical and Electronic Engineering, Imperial College London. Since September 2005, he has been with the Communications Research Group, Department of Electronic and Electrical Engineering, University of Sheffield, UK, as a lecturer. His research interests are mainly in sensor array signal processing, blind signal processing, multirate signal processing and their various applications in wireless communications, sonar, radar, satellite navigation, speech enhancement and biomedical engineering. He has now authored and co-authored more than 140 journal and conference publications, and a research monograph about wideband beamforming ("Wideband Beamforming: Concepts and Techniques", John Wiley & Sons, March 2010).